BIOCHEMISTRY
including biophysical chemistry & molecular biology
Article

Biochemistry **2010,** *49,* 4705–4714 4705
DOI: 10.1021/bi100491s

Geometry and Efficacy of Cross-Strand Trp/Trp, Trp/Tyr, and Tyr/Tyr Aromatic Interaction in a β-Hairpin Peptide[†]

Ling Wu, Dan McElheny, Takahiro Takekiyo,[‡] and Timothy A. Keiderling*

Department of Chemistry, University of Illinois at Chicago, 845 W. Taylor Street, Chicago, Illinois 60607-7061
[‡]Current address: Department of Applied Chemistry, National Defense Academy, 1-10-20, Hashirimizu, Yokosuka, Kanagawa 239-8686, Japan.

Received April 1, 2010

ABSTRACT: The Trpzip2 peptide (WTWENGKWTWK-NH_2), designed by Cochran and co-workers, contains two pairs of Trp's having cross-strand interaction and forms a stable antiparallel β-hairpin. In order to study the geometries and effects on the structure and stability of different aromatic interactions, selected tryptophan residues were substituted with Tyr to get three Trpzip2 mutants with different Trp/Trp, Trp/Tyr, and Tyr/Tyr interacting pairs. Their native-state structures were determined using two-dimensional (2D) NMR and shown to have the same cross-strand edge-to-face Trp/Trp interaction as that in Trpzip2 for the Trp/Trp pair. The analogous Trp/Tyr and Tyr/Tyr pairs also tended to have an edge-to-face geometry. The effects of specific Trp/Trp, Trp/Tyr, and Tyr/Tyr interactions on hairpin stability were studied by varying temperature and monitoring structure with electronic circular dichroism (CD) and infrared (IR) absorption spectra. IR and CD temperature variations were fit to a two-state model that yielded lower T_m values for Tyr containing mutants, indicating that Trp/Tyr and Tyr/Tyr interactions have less contribution to hairpin stability than the Trp/Trp interaction. Trp/Tyr interactions can provide significant stabilization, much greater than the Trp/aliphatic interaction, but Tyr/Tyr interactions are not as significant. Cross-strand interacting residues involving Trp with an edge-to-face orientation with Trp or Tyr had the strongest impact on hairpin stability.

β-hairpins are widely observed structural features in proteins and provide an appropriate system for theoretical modeling and structural studies which have tended to focus on design (*1*−*6*) and folding (*7*−*13*). The folded conformation of β-hairpins is principally derived from three stabilizing factors: hydrogen bonds that are formed between backbone amide groups across the strands, the interactions of side chains that bring two β-strands into close proximity, and stabilization of strand reversal enhanced by selected β-turn sequences. Considering side chain interactions, the significance of aromatics in stabilizing β-hairpin structure is now accepted, whereas the geometry and specificity of these interactions are less well established. In this study, we examine aryl/aryl interactions in a designed β-hairpin peptide. There are two dominant geometries of aryl/aryl interactions, edge-to-face (EtF) and parallel displaced (PD) stacking (*14*−*16*), with EtF geometry being more favorable for aryl/aryl interactions involving Trp or Tyr (*17*). Studies of the frequency and consequences of aromatic residue pairings in protein β-sheets can provide insights into these interactions (*18*−*25*), but significant questions still remain about Trp related interactions and their ability to impose structure in short peptide sequences.

Previous reports studying peptide hairpins suggest that aromatic interactions are excellent stabilizing agents of the secondary structure scaffold (*14*, *26*−*28*), which also affects receptor properties for these peptides (*29*). A number of β-hairpin model peptides have been designed on the basis of the stability induced by β-strand aromatic side chains interacting to form hydrophobic clusters (*1*, *27*, *28*, *30*−*37*). The location of aromatic hydrophobic clusters in the β-strand, whether near the turn or the termini, has been shown to affect β-hairpin backbone formation (*38*−*40*).

We here employ Trpzip2 (SWTWENGKWTWK) as a β-sheet template to probe different aromatic interaction geometries and further define their efficacy in stabilizing β-hairpin conformation. Trpzip2 (tryptophan zipper), as designed by Cochran and co-workers (*1*) is one of the most stable β-hairpins, resulting in a two stranded β-sheet model peptide with a hydrophobic side formed by four interacting tryptophans (Figure 1a). In Trpzip2, two pairs of edge-to-face Trp/Trp interactions (residue pairs: 4−9 and 2−11) are formed, which subsequently couple through a face-to-face Trp/Trp interaction (residue pair: 2−9). We have previously reported studies of equilibrium and kinetic unfolding of a Trpzip2 hairpin, having all four Trp's but including minor modifications for isotopic labeling (*41*, *42*). Additionally, we also reported studies of Trpzip2 related sequences where the three sets of Trp/Trp interactions are pairwise substituted by Val residues to study aliphatic−aromatic hydrophobic interaction (*40*). In this new study, we substitute two Trp's with Tyr's at variable positions to probe the effect of aromatic pairs involving Tyr and Trp residues at different positions on the β-hairpin and to develop detailed geometries for these various aryl/aryl interactions. We previously carried out a thermodynamic study on similar mutants of another hairpin, Trpzip1, that has a different β-turn (Gly-Asn) and markedly less stability, resulting in different sets of behaviors (*43*).

[†]This work was funded in part by a grant from the National Science Foundation (CHE07-18543).
*To whom correspondence should be addressed. Tel: 1-312-996-3156. Fax: 1-312-996-0431. E-mail: tak@uic.edu.

Published on Web 04/27/2010

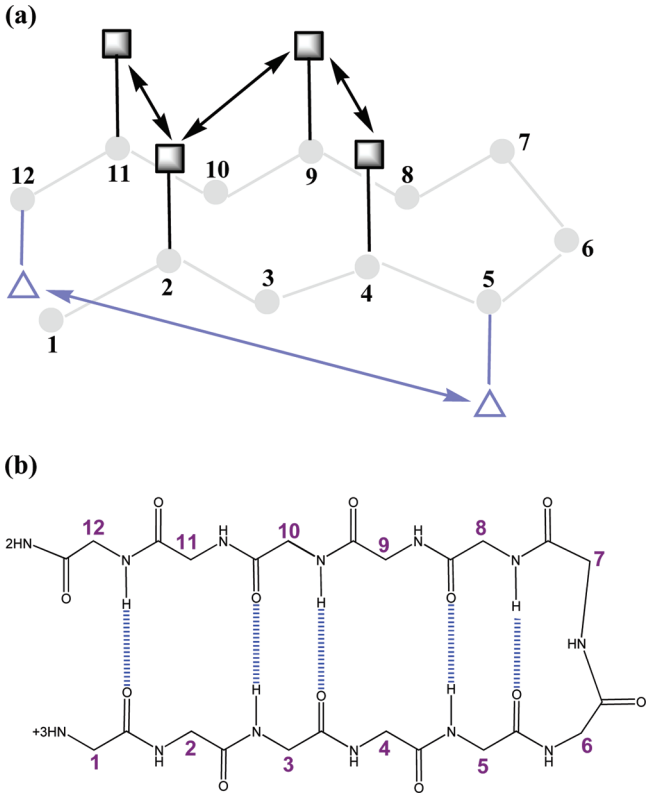

FIGURE 1: (a) Schematic representation of Trpzip2-like peptide showing possible modes of aromatic interactions between residues 2, 4, 9, 11 (above the β-strands). The light blue arrow indicates a salt bridge between E5 and K12 (below the β-strands) that is detected in our NMR structures. (b) Schematic representation of a 12-mer β-hairpin marked with expected cross-strand H-bonds.

Table 1: Comparative Sequences of Peptides Used for This Study

peptide	sequence[a]	backbone geometry
Trpzip2	SWTWENGKWTWK-NH_2	hairpin
WYWY	SWT**Y**ENGKWT**Y**K-NH_2	hairpin
WYYW	SWT**Y**ENGK**Y**TWK-NH_2	hairpin
YWWY	S**Y**TWENGKWT**Y**K-NH_2	hairpin
W2W9[b]	SWTVENGKWTVK	random coil
W2W11[b]	SWTVENGKVTWK	hairpin
W4W9[b]	SVTWENGKWTVK	hairpin

[a]Bold font and underlining represent the mutated position. [b]Sequences previously studied and used for comparison in conclusions.

We here report conformational analysis and thermal stability studies for three tyrosine mutant peptides based on β-hairpin Trpzip2, whose sequences are listed in Table 1 and diagramed in the Supporting Information, Scheme S1. All peptides studied here are expected to support five intramolecular cross-strand hydrogen bonds in an ideal β-hairpin conformation (Figure 1b). Using two-dimensional (2D) NMR structural studies, we establish side chain orientations for closely interacting Trp/Trp, Trp/Tyr, and Tyr/Tyr pairs at the non-hydrogen bonding positions for this designed β-hairpin in aqueous solution. These are correlated to the hairpin backbone structure and stability, as obtained through temperature-dependent spectral analyses, to demonstrate the effectiveness of the various pairs for hairpin formation. Combined with our previous work, which addressed hydrophobic effects through Trp-Val mutation, we compare the effects of hydrophobic clustering with and without aromatic interaction on this β-hairpin model.

EXPERIMENTAL PROCEDURES

Peptide Synthesis and Purification. All peptides were synthesized in house using standard Fmoc-based solid-state synthesis methods. In this process, four equivalents of amino acid were activated with TBTU, HOBt (final concentration of 0.25M), and diisopropylethylamine (DIEA) (final concentration of 0.5 M). A stepwise coupling of each amino acid was obtained using standard solid-phase Fmoc coupling chemistry. Once the synthesis was complete, the peptide was removed from the solid-phase Rink Amide MBHA resin using a cleavage cocktail (by dissolving in 88:5:5:2 TFA/phenol/water/TIPS for 3.5 h). Crude peptides were isolated by precipitation into 10 volumes of cold ether, purified by reverse phase HPLC (VYDAC 218TP510 reversed-phase column), and characterized by MALDI-MS (expected M_w, 1561.7; obtained M_w, 1560.9). All synthesis reagents and resin were purchased from AnaSpec Inc. Ultimate characterization by the spectral studies described below confirmed the synthesis and the formation of a β-hairpin structure in each case.

NMR Spectra and Structure Analysis. TOCSY and NOESY spectra were acquired on a Bruker AVANCE 800 MHz spectrometer for TZ2, WYWY, WYYW, and YWWY. All peptide concentrations were ~4 mM in a solution of 20 mM phosphate buffer (90% H_2O and 10% D_2O) at pH 5.8. Spectra were acquired at 281 K, as calibrated with methanol, in order to push the equilibrium more toward a folded population. 2D NOESY were acquired (mixing times = 80 and 300 ms) with 12 PPM sweep widths, 2048 × 1024 complex points in $t_2 \times t_1$, and 16 scans per increment. 2D TOCSY were acquired under similar conditions with DIPSI2 mixing of 70 ms and an RF field of 8 kHz. The 2D NMR spectra were processed within NMRPipe (*44*) and viewed/assigned in NMRView (*45*).

Temperature-dependent chemical shift variation of the aromatic ring proton resonances and backbone amide protons in WYWY were measured on a Bruker DRX 500 MHz spectrometer. The one-dimensional (1D) ^{1}H NMR spectra were acquired with 32 scans at every 5 K interval over the 285 K to 345 K temperature range. All 2D and 1D experiments incorporated water suppression through gradient selection and excitation sculpting (*46*).

The NOESY peaks were manually selected and assigned with CYANA 2.0 (*47*). The 100 lowest energy structures were selected from an ensemble of 500 and further refined by restrained MD using a previously described methodology within AMBER 8 (*48*). We used the ff99sb force field (*49*) plus the SHIFTS restraint (*50*) for the Trp rings with a force constant of 2 kcal/mol. The resulting 20 unique structures with the lowest AMBER and restraint violation energies were subjected to structure validation within PROCHECK_NMR (*51*).

Circular Dichroism Spectroscopy. For CD experiments, peptide solutions were prepared at ~0.2 mg/mL (~0.13 mM) in 20 mM phosphate buffer (pH 7). Far-UV CD spectra were acquired between 185 and 260 nm at 50 nm/min, with a 1 nm bandwidth and 2 s response time on a JASCO J-810 spectrometer using a 1 mm quartz cell (Starna, Inc.). Determination of sample concentration was based on absorbance at 280 nm (Trp ε_{280}, 5560 M^{-1} cm^{-1}; Tyr ε_{280}, 1200 M^{-1} cm^{-1}). Final spectra were recorded as an average of eight scans and baseline subtracted.

Variable-temperature experiments were done with a 1 °C/min ramp speed and a 5-min equilibration time, the temperature controlled by flow from a water bath (Neslab RTE7DP). Spectra over the range of 5−85 °C (in steps of 5 °C) were obtained for the

sample and buffer (for baseline subtraction) under identical experimental conditions. No smoothing was performed on the spectra. The CD amplitude variation with temperature was fit to a two-state model that used linear folded (low temperature) and flat unfolded (high temperature) baselines with $\Delta C_p = 0$ since this gave the most reliable fits. Other models were tested and are compared as described in the following sections.

Infrared Spectroscopy. Purified peptides were lyophilized twice against 0.1 M DCl/D_2O solution (both DCl and D_2O obtained from Sigma) to remove TFA counterions remaining from the peptide synthesis and then redissolved in D_2O, neutralized by NaOD, and lyophilized again. Peptide solutions for IR studies were prepared in a range of concentrations, ~15−25 mg/mL (~10−17 mM), by dissolving lyophilized peptides in 20 mM deuterated phosphate buffer in D_2O to get pH ~7.

IR spectra were acquired on a DigiLab FTS-60A spectrometer (Randolf, MA). Peptide solutions were sealed in a homemade demountable cell with CaF_2 windows separated by a 100 μm Teflon spacer. Sample and background spectra were collected at 4 cm^{-1} resolution with a zero-filling factor of 8. Temperature-variation experiments were conducted by placing the sample in a homemade cell holder stabilized at selected temperatures from 5 to 90 °C by flow from a bath (Neslab RTE 111). The sample was heated in 5 °C steps and equilibrated, and then 940 coadded scans were accumulated before the next temperature step.

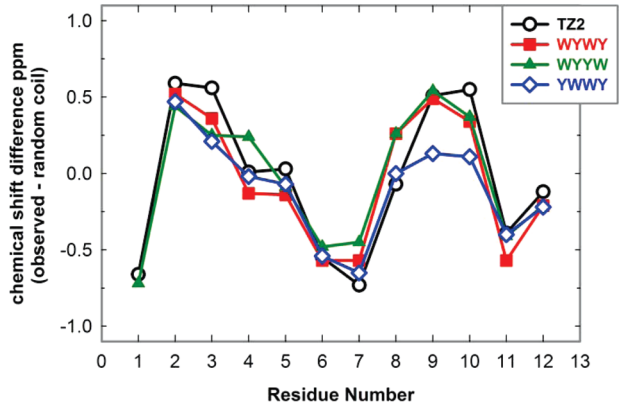

FIGURE 2: Plot of the variation of $C_\alpha H$ chemical shifts with respect to random coil chemical shifts in TZ2 (open black dot), WYWY (filled red square), WYYW (filled green triangle), and YWWY (open blue diamond).

RESULTS AND DISCUSSION

Backbone Conformations of Tyrosine Mutant Peptides. All of the tyrosine mutant peptides have solubility comparable to that of TZ2. NMR studies were carried out in aqueous solution, and sequence specific assignments for the three peptides were achieved using a combination of 2D spectra from TOCSY and ROESY experiments (see Table S1 in Supporting Information for chemical shift data). Hα chemical shift deviations (CSD) from random coil values provide a method for identifying sequence segments having β-hairpin formation (*34*, *52*−*56*). The backbone chemical shift index values for the Cα-Hs of the three tyrosine mutant peptides were compared to those of Trpzip2 (*41*) by computing the observed shifts relative to random coil shifts for individual residues. All three mutants showed qualitatively the same pattern as did the original Trpzip2 β-hairpin (Figure 2), with residues 2−3 and 9−10 having large downfield shifts, consistent with their forming β-strand segments, and residues 6−7 having large upfield shifts, indicating α-like or β-turn local conformations. These consistent Cα-H backbone patterns indicate that all three mutants form β-hairpin structures similar to what we and others have found for TZ2 (*1*, *41*). However, the positive shifts of residues 9−10 for YWWY are weaker than those for WYWY or WYYW, which may suggest a less extensive or less stable β-structure for that hairpin.

This stability difference probably results from YWWY having a Tyr/Tyr pair near the termini instead of the more strongly interacting Trp/Trp pair, which is consistent with Tyr/Tyr being less efficient in locking two β-strands into a cross-strand position, as expected. As a consequence, YWWY might be expected to have less extended β strands than do TZ2, WYWY and WYYW. Stronger tertiary aromatic interactions formed by Trp/Tyr interactions do improve the stability of the neighboring backbone structure.

Aromatic Interactions in Cross-Strand Pairs. In order to study different side chain interactions and their corresponding tertiary geometries for our mutant peptides, the TOCSY NMR spectra of all three mutants for the labeled characteristic aromatic protons indicated in Figure 3 were used. In mutants WYYW and YWWY, a clear pattern of three cross-peaks associated with the HZ2, HH2, and HZ3 protons on the indole ring coupled to HE3 for Trp11 in WYYW and for Trp4 in YWWY indicates that these particular residues are oriented in the edge position of an edge-to-face pair interaction geometry.

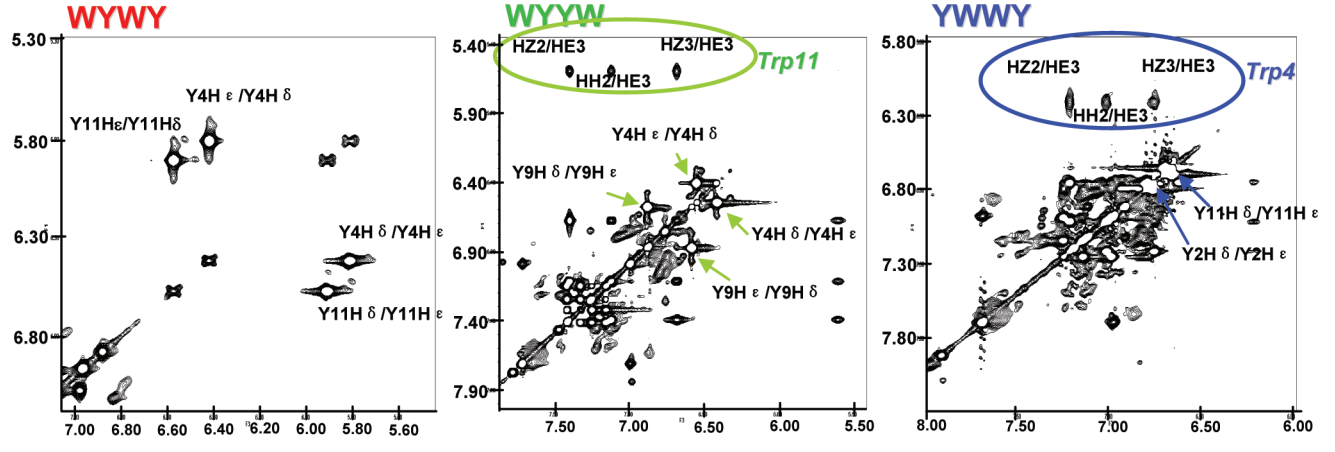

FIGURE 3: Partial expansions of the aromatic region (about 5−8 ppm) in the TOCSY NMR spectra of WYWY, WYYW, and YWWY recorded at 283 K. Some assignments are labeled. Circles indicate diagnostic cross-peaks for edge-to-face Trp-Trp pairs.

Table 2: Observed Chemical Shifts of Hβ and Trp HE3, and Tyr Hδ/Hε, and Comparison of NOE Numbers for Tyr Rings

atom	WYWY[a]	WYYW[a]	YWWY[a]	TZ2[a,b]
2 HE3 or (Hδ/Hε)	7.5	7.3	6.8/6.7	7.5
4 HE3 or (Hδ/Hε)	**5.8/6.4**	6.4/6.5	**6.2**	**5.5**
9 HE3 or (Hδ/Hε)	7.7	6.9/6.6	7.2	7.3
11 HE3 or (Hδ/Hε)	**5.9/6.5**	**5.6**	6.7/6.6	**5.3**
2 Hβ	3.1/3.3	3.1/3.1	2.3/2.5	3.0/3.1
4 Hβ	**0.8/2.3**	2.8/2.6	**2.4/3.0**	**3.0/2.1**
9 Hβ	3.1/3.3	2.9/2.8	2.8/3.0	3.3/3.0
11 Hβ	**1.1/2.3**	**2.8/2.2**	2.8/2.8	**2.8/2.0**
position	# of Tyr NOEs			
2			15	
4	35	36		
9		40		
11	27		11	
total	62	76	26	
rmsd (bb/sc)	0.25/0.57	0.20/0.57	0.39/0.81	

[a]Bold font indicates the edge position on the ring. [b]Data of TZ2 are from ref *1*.

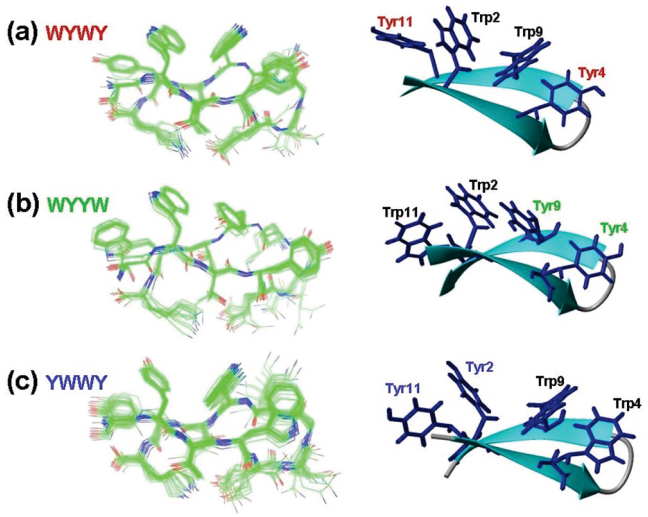

FIGURE 4: (Left) Peptide backbone overlap of the 20 best NMR structures determined for (a) YWWY, (b) WYYW, and (c) WYWY. (Right) Ribbon structures showing the aromatic side chain interaction (pairwise) layout. Other side chains are removed from the figure for clarity.

In WYWY, although there are two pairs of edge-to-face aromatic interactions, we do not see this pattern for tryptophan. This is because two tryptophans are both in the face position and not in the edge position (see structure analysis below), and the tyrosines which are in the edge position lack this characteristic proton pattern. Instead, when tyrosine is in an edge-like position, those side chain protons projected at the neighboring face-positioned aromatic rings are shielded so that the Hδ and Hε protons have split cross-peaks due to this asymmetrical shift, as shown in WYWY and WYYW. Apparently, the Tyr Hδ and Hε in WYWY have more ring shielding than for the Tyr in WYYW and hence exhibit much larger splitting.

By contrast, Tyr2 and Tyr11 in YWWY only show a single diagonal coupling peak for Hδ and Hε, which indicates that these tyrosines are not in fixed interacting positions or significantly shielded by a neighboring aryl ring current, and thus they exhibit degenerate Hδ and Hε coupling peaks. In the next section, this particular pattern is correlated with tertiary aromatic structure.

To further examine and characterize the above aromatic interactions, in Table 2 we list observed Hβ chemical shifts for all aromatic residues in the original β-hairpin TZ2 and in the three tyrosine mutants. Hε3 for all of the tryptophan indole rings and Hδ/Hε for all tyrosines are also listed. In the bottom part, the numbers of associated NOEs are identified for the tyrosine rings. Consistent with TZ2 having two pairs of Trp/Trp interactions coupled edge-to-face with the edge-positioned Trp at residues 4 and 11, Trp11 in WYYW and Trp4 in YWWY show a clear upfield shift (5.2−6.2 ppm) for HE3, which is much smaller than the unperturbed HE3 value (~7.5 ppm). Similarly, when tyrosine is located in the edge position of an edge-to-face interacting pair, its Hδ/Hε protons show a large nondegeneracy (>0.5 ppm) as can be seen for Tyr4 and Tyr11 in WYWY. This phenomenon was also noticed in other designed β-hairpins containing Tyr/Tyr interaction with facing side chain geometry (*14*). These unusual shielding chemical shifts result from the ring current effects characteristic of the particular orientation of two aromatic rings. Also, Hβ for the interacting aromatic residues at the edge position exhibits a characteristic large splitting for both Trp (>0.6 ppm) and Tyr (>1.2 ppm). All of the chemical shifts representing the edge position residues listed in Table 2 are marked in bold font. The number of NOEs identified that are associated with Tyr in YWWY is much less than that for WYWY and WYYW, indicating that the Tyr/Tyr pair in YWWY either has weaker interactions or a less fixed tertiary geometry or both.

NMR-Derived Structures of Mutant Peptides. Optimizations of the solution structures to fit our NMR data were undertaken to confirm these experimental observations. A simulated annealing protocol was used in conjunction with constraints based on NMR chemical shift and NOE data to generate a number of low-energy structures for these β-hairpins. An overlap of the 20 lowest-energy structures obtained from this analysis for all three tyrosine mutants, WYWY, WYYW, and YWWY, respectively, are shown in Figure 4a, b, and c, left side. Structures of WYWY and WYYW show a high level of overlap, while YWWY structures display relatively more fraying both for the backbone and side chain positions. Each mutant sequence shows some population of structure with a different turn conformation (1 for WYWY, 2 for WYYW, and 4 for YWWY out of 20). The detailed ^{1}H chemical shifts of all mutants in 20 mM phosphate buffer (H_2O with 10% D_2O) and relevant information used for the structure determinations are listed in Table S1 of Supporting Information. To more clearly compare aromatic side chain interactions in these three hairpins, a set of corresponding ribbon drawings are shown in Figure 4a, b, and c, right side, that includes only the aromatic side chain layout for a typical example best structure for each mutant.

The side chain orientations of the Trp pairs in WYYW and YWWY shown in Figure 4 closely follow those determined for the Trpzip2 NMR structures (*1*, *41*, *57*). They maintain the relative Trp geometries previously reported for TZ2 with a high degree of fidelity, and experimental CD patterns arising from these coupled Trp geometries are identical (see below). Both pairs are oriented with one Trp indole ring packing edge-on to the face of the other Trp indole ring. By contrast, side chain structures dependent on Tyr interactions exhibit more complexity. The Tyr9 side chain in WYYW is located between Trp2 and Tyr4, and develops strong NOEs with both residues. As a result, it forms a shift-stacked conformation with Trp2 and a T-shape one with

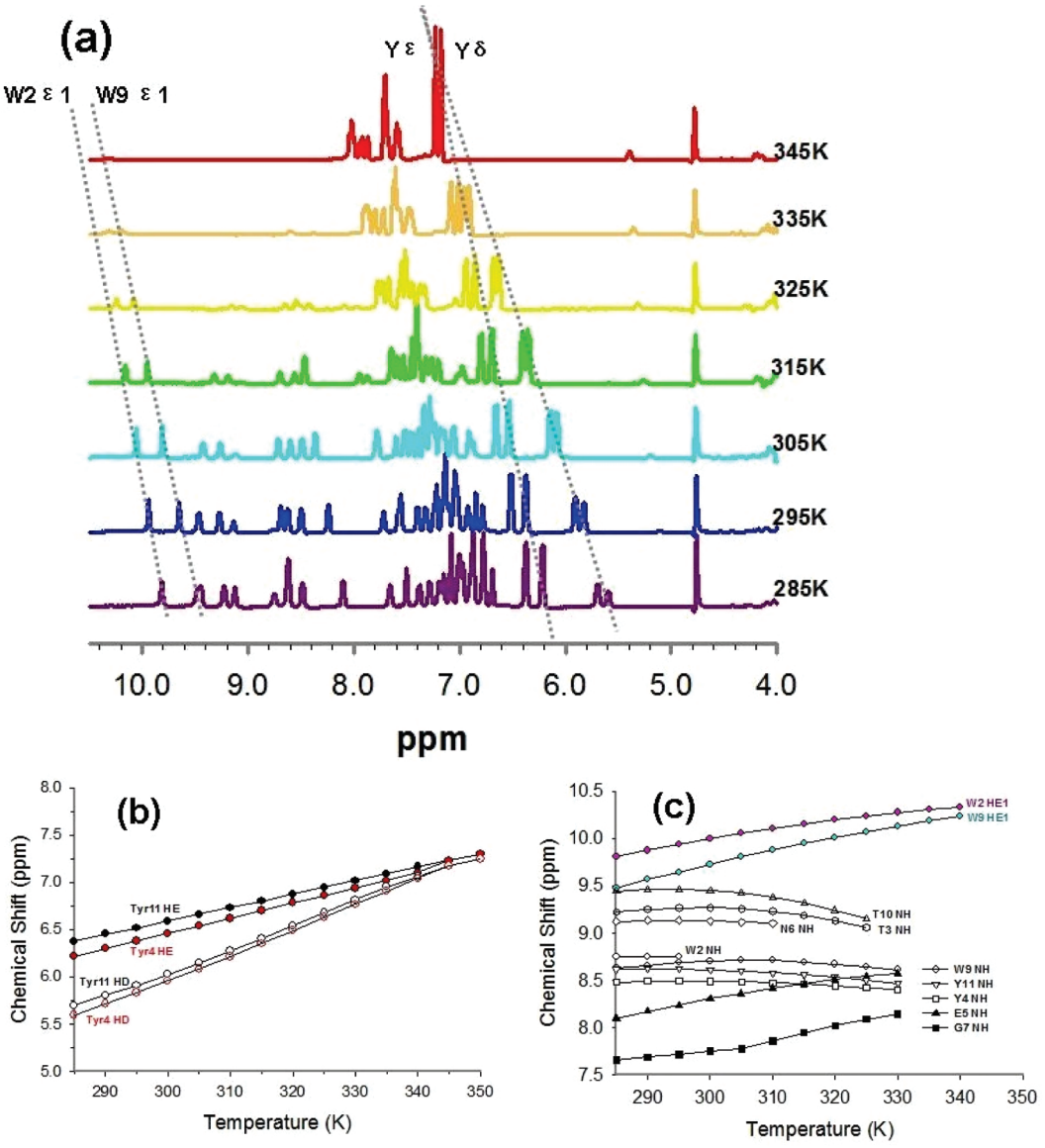

FIGURE 5: (a) Temperature-dependent chemical shift variation of the aromatic ring proton resonances of Tyr4 and Tyr9, and backbone amide protons in WYWY. (b) Hε1 of tryptophan and Hδ/Hε of tyrosine monitor side chain interaction unfolding with increasing temperature, and (c) backbone N−H resonances probe exposed (E5 and G7) vs hydrogen bonded amides.

Tyr4. Although the Tyr/Tyr pair in the YWWY structure exhibits a shifted edge-to-face geometry, it does not have measurable NOE (Table 2) interactions between the two tyrosine rings and shows a more disordered structure.

WYWY has two pairs of Trp/Tyr pairs, each adopting an edge-to-face geometry, with the Tyr ring oriented in the edge position of each pair. This pattern reflects the Trp/Trp pairs in WYYW and YWWY but is different from the Trp/Tyr pairs in those sequences. In the WYWY Trp/Tyr interaction pairs, Hβ of Tyr4 and Tyr11 point toward the Trp indole ring and result in a large upfield chemical shift for one Hβ proton (Table 2). Finally, a salt bridge appears to form between Glu5 and Lys12 on the hydrophilic side of the β-strands in the structures of all three mutant peptides. All of these conformational characteristics are consistent with our experimental optical spectroscopic data, as detailed below.

Temperature dependencies of the chemical shifts were also observed for the backbone amide and aromatic protons in the WYWY peptide (Figure 5a). Extracted chemical shifts as a function of temperature for Hδ/Hε of Tyr4 and Tyr11, Hε1 of Trp2 and Trp9, and all amide proton resonances are summarized in Figure 5b and c. Because this data later yielded poor fits with our thermodynamic analyses, presumably due to the convolution of normal chemical shift temperature dependencies with conformational change effects, similar measurements were not pursued for the other peptides. Chemical shifts of the aromatic proton resonances (in color) show obvious downfield shifts upon structure relaxation as a function of increasing temperature. Tyr Hδ/Hε shifts exhibit thermal dependencies similar to those of the Trp Hε1 shifts, which indicate that all four aromatic side chains may unfold synchronously through one correlated mechanism. The relative insensitivity and opposite thermal trend of the chemical shifts of the NH resonances for residues T3, Y4, W9, T10, and Y11 (open symbols), which are distributed on two β-strands, is consistent with their dependence on the cross-strand hydrogen bonded status. By contrast, the NH resonances of E5 and G7 (solid symbols), which are at the turn sequence, show more pronounced thermal shifts. This might be correlated with less stability in the turn as would be consistent with our identification of a population of other turn conformations and could be

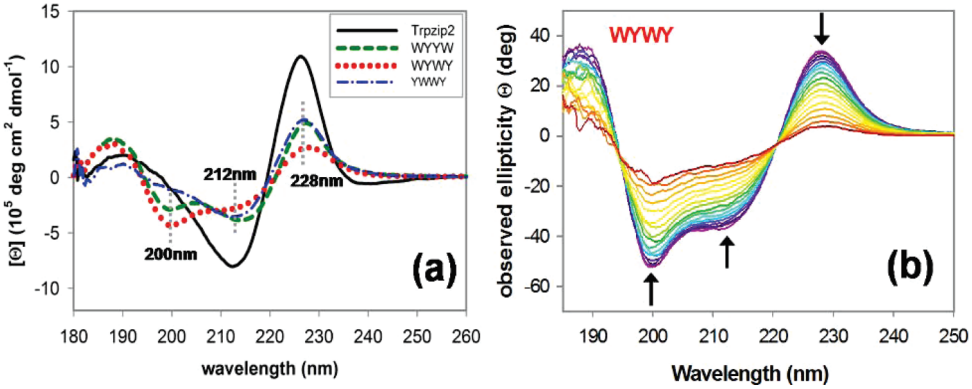

FIGURE 6: (a) CD spectra of Trpzip2 and tyrosine mutant peptides WYWY, WYYW, and YWWY at 5 °C. Peptide concentration is ~0.2 mg/mL in 20 mM phosphate buffer (pH 7), and path length is 1 mm. The vertical axis was corrected to molar ellipticity on a molecular basis using solution concentrations determined by UV absorbance at 280 nm. Trpzip2 (black line), WYWY (red dot), WYYW (green diamond), and YWWY (blue dash line). (b) Temperature-dependent CD spectra of tyrosine mutant peptide WYWY measured from 5 to 85 °C. Color changes indicate increasing temperature, from violet (cold) to red (hot).

a characteristic of solvent exposed residues such as G7 in an ideal β-hairpin conformation.

Implications for Tertiary Structure Aromatic−aromatic Pairs by CD. Far-UV CD is often used for rapid assessment of folded peptide backbone conformations in solution. For Trpzip2, an unusual CD spectrum, with intense exciton-coupled Trp bands at 212 and 228 nm can instead be used to monitor the cross-strand (tertiary) interaction between the aromatic chromophores (*1*, *40*). Both WYYW and YWWY, with one pair of cross-strand edge-to-face coupled Trp's, have the same type of strong negative−positive Trp $\pi-\pi^*$ exciton-coupled bands as seen in Trpzip2 but result in a little less than half the intensity (see Figure 6a). WYWY, which has a diagonal cross-strand face-to-face Trp/Trp interaction, also exhibits exciton-coupled Trp bands in CD but with much less intensity than for WYYW or YWWY. This is consistent with the Trp/Trp edge-to-face aromatic interaction having a stronger characteristic CD spectrum than the Trp/Trp face-to-face layout, as we have previously predicted using TD-DFT computations of the CD for various Trp/Trp pairs (*58*).

Interestingly, WYWY and WYYW show an extra negative exciton band at 200 nm, but this is not evident in the Trpzip2 or the YWWY CD spectra. Presumably, this band arises from Tyr/Trp interactions which are strong in WYWY and WYYW but less so in YWWY. In WYWY, the short W−Y distances are 3.6−4 Å, while in WYYW, the geometry changes, but the distance is ~4.3 Å, and the W−Y interaction in YWWY is > 5 Å . The 200 nm negative band of WYWY is more intense than that of WYYW, which may due to WYWY having two Trp/Tyr edge-to-face pairs, while WYYW only has one pair, which in addition has a shift-stacked conformation. The shape and position of the aromatic chromophore exciton bands in the CD spectra appear to account for the different aromatic interaction types, and their relative band intensities also reflect the numbers of interacting aromatic pairs.

Calculated CD spectra obtained from TD-DFT model calculations of aromatic rings constrained to the relative geometries in WYYW, YWWY, and WYWY are qualitatively consistent with experimental data. As previously reported for other similar calculations (*58*), the Trp/Trp edge-to-face pairs, 2−11 in WYYW and 4−9 in YWWY, yield a dominant couplet CD at ~280 nm. The Trp/Tyr interacting pairs with edge-to-face geometry in WYWY also are both predicted to give rise to negative−positive exciton bands at ~195 nm and ~200 nm, yielding a CD shape similar to that of the Trp/Trp edge-to-face CD bands, except blue-shifted by ~10 nm. We assign this to the experimentally observed extra negative band at 200 nm. However, when summed, such calculated modeling based on pairwise interactions does not quantitatively reflect the experiment for these mixed side chain hairpin CD spectra. This suggests that our initial, vacuum computed Tyr-Trp energy shifts are probably in error and that the shift may affect the resulting coupling. Finally, at this point, these preliminary TD-DFT calculations do not adequately model Tyr/Tyr interactions, which may be indicative of a solvation problem or may be due to fluctuation of Tyr side chains in the experimental case.

Table 3: Thermodynamic Parameters for the Two-State Model Fit of Thermal ECD Data for Trpzip2 and Its Tyr Mutants

peptide	band position (nm)	T_m (K)	ΔH (kcal·mol^{-1})	ΔS (cal·mol^{-1}·K^{-1})
Trpzip2	226.8	352 ± 2	17 ± 2	48.3
	212.6	349 ± 2	18 ± 2	50.6
WYWY	228	346 ± 1	14 ± 1	40.8
	212	345 ± 2	15 ± 2	43.1
	200	343 ± 3	21 ± 4	60.3
WYYW	227.4	330 ± 1	15 ± 1	45.1
	214	329 ± 1	14 ± 1	43.7
	200.2	337 ± 14[a]	9 ± 5	25.5
YWWY	227	336 ± 1	15 ± 1	45.8
	212.6	339 ± 2	16 ± 2	46.0

[a]Large fitting error for the 200.2 nm band of WYYW.

The thermal stability of these aromatic interactions in phosphate buffer was monitored by variable-temperature CD, and representative data for WYWY is illustrated in Figure 6b. With increasing temperature from 5 to 85 °C, both the strong negative−positive Trp-Trp exciton-coupled bands at 212 and 228 nm and the negative Tyr-dependent band at 200 nm collapse at higher temperatures, consistent with a loss of Trp/Trp and Trp/Tyr or Tyr/Tyr interactions resulting from unfolding of the tertiary structure.

The intensity losses of the aromatic exciton bands (200 nm, 212 nm, 228 nm) with increasing T were measured to yield

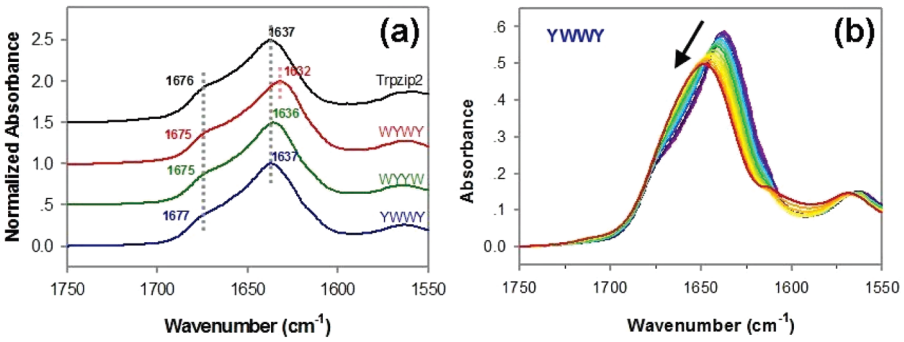

FIGURE 7: (a) FTIR spectra of Trpzip2, WYWY, WYYW, and YWWY measured in 20 mM deuterated phosphate buffer at 5 °C and a path length of 100 μm. Spectra were normalized to a maximum absorbance of 1. Trpzip2 (black), WYWY (red), WYYW (green), and YWWY (blue). (b) Temperature-dependent IR spectra of tyrosine mutant peptide YWWY measured from 5 to 85 °C. Color changes and arrow direction indicate increasing temperature, from violet (cold) to red (hot).

thermal transition curves, which were then fit to a two-state model that used a linear folded and flat unfolded baseline with $\Delta C_p = 0$ (*40*, *41*). The fitting results including transition temperatures, T_m, and corresponding thermodynamic parameters, ΔH and ΔS, are listed in Table 3. All data were also fit to a two-state model with linear baseline for both folded and unfolded states, and consistent results were obtained for WYWY, WYYW, and YWWY, but these had larger errors (Supporting Information, Table S2). Considering the inclusion of ΔC_p in the model, we found that all fit values were zero within the error and found much larger errors for T_m, as we have shown before for other Trpzip2 variants (Supporting Information, Table S4) (*40*, *41*). Of the three mutations, the WYWY errors with linear−linear baseline were the largest, presumably reflecting the lower degree of interaction and hence CD (signal strength). Because TZ2 exhibits a more stable hairpin at high temperatures, which results in an unfinished transition curve approaching the unfolded state, a linear−linear baseline model results in the unfolded baseline mimicking the transition and not the temperature dependence of the unfolded state (for an example, see Supporting Information, Figure S1). Thus, the TZ2 CD data end up being fit to physically unrealistic T_m values in addition to having relatively high errors with linear unfolded baselines. The flat baseline tends to stabilize the model, yielding consistent results and a sensible unfolded temperature dependence for the CD intensity, but it certainly could cause some small errors. The consistency of our results for linear and flat baselines, when they both yield sensible transition curves, shows that the use of a flat baseline has a minimal effect on T_m and ΔH.

From a comparison of T_m values, we can see that the Trp/Trp interactions in Trpzip2 are the most stabilizing in that they yield the highest T_m at ~350 K. For the Trp/Trp exciton bands and the Trp/Tyr band for WYWY, comparable T_m values are found, which are ~5 K lower than that of Trpzip2. This indicates that the Trp/Tyr edge-to-face interaction is less stable than the Trp/Trp edge-to-face interaction, but nonetheless it provides enough energy to allow two cross-strand Trp/Tyr pairs to stabilize the hairpin structure. By contrast, the unique, cross-strand Trp/Trp interaction pairs in WYYW (T_m ~330 K) and YWWY (T_m ~336 K) show less stability than do these aromatic groups in Trpzip2 (less than half the CD intensity, and lower T_m) and lower T_m than provided by the ensemble of Trp/Tyr and Trp/Trp interactions in WYWY. These observations suggest that the cross-strand aromatic interactions are not independent but act in concert to oppose the tendency of the hairpin to open. Furthermore, Trp2 in WYYW has a strong and unique (in this series) shift-stacked interaction with Tyr9. Surprisingly, this Trp/Tyr interaction appears to disrupt the potential Tyr4-Tyr9 interaction, although WYYW still has a significant Tyr-based CD band. Possibly as a consequence, the Trp/Trp interaction is destabilized compared to the Trp/Trp interaction in YWWY.

Peptide Secondary Structure Stability Studies by IR. IR spectra of the amide I′ mode (C=O stretch) primarily reflect the dominant secondary structure forms in a peptide via frequency shifts. All three tyrosine mutants and the original Trpzip2 show similar amide I′ (D_2O solution) band shapes at 5 °C, yielding a broadened, intense band with a maximum at ~1637 cm^{-1} and a weak shoulder at ~1675 cm^{-1} (Figure 7a). These band dispersions are consistent with the formation of a partial antiparallel β-sheet cross-strand interaction. WYWY is an exception in that the lower frequency component is shifted further down by ~5 cm^{-1}, which probably arises from the structure, in that the β-strands are flattened. The NMR structure of WYWY shows less twisting particularly at the termini, which can enhance amide I exciton coupling and hence splitting of the high and low frequency amide I components in β-sheet structures (*59*).

In order to correlate the secondary structure stability (IR monitored), in particular for the β-strand, with the related tertiary structure stability (CD monitored), these peptides were studied with variable-temperature IR. The frequency of the amide I absorption maximum exhibits a blue shift as temperature increased from 5 to 90 °C (see Figure 7b), corresponding to a secondary structural change from hairpin (β-strand) to a mostly disordered structure. From the variable-temperature IR, the intensity change at the frequency of the maximum absorption was extracted and fit for thermal analyses as described in our previous studies (*40*, *41*), and the results are summarized in Table 4. Fitting results obtained using a linear baseline for both the folded and unfolded states are compared with the linear−flat baseline model in Supporting Information (Table S3). Although the WYWY fits are similar with both baseline models, with the linear−linear baseline model the TZ2, WYYW, and YWWY IR data result in much lower T_m and ΔH values plus bigger errors because these secondary structure transitions do not establish a clear, stable unfolded state at high temperatures. In such a case, the linear unfolded baseline is fit to the transition and not the normal temperature-dependent IR absorbance, as discussed above for the CD result in TZ2. The consistency of the WYWY results with both models (Table S3, Supporting Information) shows that our use of a flat baseline is a reasonable approximation for these unfinished transitions.

Consistent with the CD tertiary stability results, all mutants are less stable than is Trpzip2 in terms of secondary structure

Table 4: Thermodynamic Parameters for the Two-State Model Fit of Thermal IR Data for Trpzip2 and Its Tyr Mutants

peptide	band position (nm)	T_m (*K*)	ΔH (kcal·mol^{-1})	ΔS (cal·mol^{-1}·K^{-1})
Trpzip2	1637.5 cm^{-1}	352 ± 3	15 ± 2	42.8
WYWY	1632.2 cm^{-1}	338 ± 2	19 ± 3	55.9
WYYW	1635.6 cm^{-1}	331 ± 2	13 ± 2	40.2
YWWY	1637 cm^{-1}	331 ± 4	11 ± 2	34.1

Table 5: Comparison of the T_m Values for the Secondary Structure (FTIR data) and Tertiary Structure (ECD data) Change for Trpzip2 and Its Tyr and Val Mutants

tyrosine(Y) mutants			valine(V) mutants		
Peptide	FTIR (K)	CD (K)	peptide	FTIR (K)	CD (K)
WYWY	338 ± 2	346 ± 1	W2W9	341 ± 5[a]	N/A[b]
WYYW	331 ± 2	330 ± 1	W2W11	332 ± 2	347 ± 4
YWWY	331 ± 4	336 ± 1	W4W9	326 ± 7	342 ± 7

[a]Extracted amide I′ IR band of W2W9 represents the random coil conformation. [b]W2W9 has no detectable Trp-exciton bands in CD.

(IR change). In contrast to the CD result, where the T_m values for the Trp/Trp interaction suggested that it was more stabilizing in YWWY than in WYYW, the T_m values for the β-strand secondary structure of these two peptides obtained from IR intensity changes are the same (331 K), and the ΔH values are equivalent (12 kcal/mol). Furthermore, the two Trp/Tyr plus the Trp/Trp aromatic interactions in WYWY result in more stability both for secondary (IR) and tertiary structure (CD) than found for WYYW and YWWY. This is consistent with WYWY having a lower frequency amide I exciton component, which generally indicates a more extended (or flatter) β-sheet-like structure.

CONCLUSIONS

The initiation of folding for the Trpzip2 β-hairpin peptide is believed to be driven by a hydrophobic collapse in which the apolar aromatic residues interact with each other and eliminate waters of solvation. Corresponding mutants with various hydrophobic and aromatic interactions (Trp/Trp, Trp/Tyr, Tyr/Tyr as well as Val/Val, and Val/Trp) are good models for differentiating the contribution of these interactions toward folding and stability. Additionally, these peptides provide the basis for the study of the preferred modes of association and packing of specific aromatic residues in protein. The ability of cross-strand Trp/Trp interactions to stabilize hairpins was a driving force for the development of Trp-zipper peptides, and the advantages of aromatic interactions in developing such structures have been studied (*1*, *27*, *28*, *60*). In previous studies from our lab, we analyzed the impact of substituting the Val-Val hydrophobic interaction (*40*). In this work, aromatic interactions between Trp and Tyr residues are explored instead using the Trpzip2 model β-hairpin. Comparison of transition temperatures as indicators of secondary and tertiary structure stability when extracted from thermal IR and CD data, respectively, are summarized in Table 5 for all mutants that we studied.

The W2W9 mutant with Val parallels the WYWY sequence and would have Val/Trp interactions, but does not form a hairpin; thus, its T_m values are not useful for comparison. The lack of hairpin formation in W2W9 does confirm the weakness of an aliphatic−aromatic cross-strand coupling. Indirectly, the difference suggests that a single stack-shifted aromatic interaction is insufficient for hairpin formation in contrast to a single edge-to-face interaction, which is sufficient, as shown by the stable hairpin structures obtained for W2W11 and W4W9 (*40*). The comparison of structures and thermodynamics for these related peptides adds to the understanding of aryl and aliphatic hydrophobic interactions and their efficacy in enhancing protein stability.

Tertiary Aromatic Interaction. Both this and our previous study indicate that a single Trp/Trp edge-to-face interaction along with another hydrophobic pair on the same side of the hairpin can locally stabilize a cross-strand structure. Trpzip2 with two such interactions, thus, has the highest stability of the related peptides in both the Tyr and Val substitution studies. While aliphatic−aromatic interaction alone is inadequate, an edge-to-face heteroaromatic interaction is sufficient for strand stabilization in a hairpin. In WYWY, we substitute an edge Trp with an edge Tyr and maintain two Trp/Tyr edge-to-face interactions, which result in comparable or even more tertiary interaction stability than for single Trp/Trp edge-to-face pairs. There is also an impact upon the secondary structure, but the difference is less dramatic.

However, the edge-to-face Trp/Trp pairs in WYYW and YWWY result in less stable tertiary interactions (T_m from CD) than found for the corresponding Val mutants, W2W11 and W4W9, and an inversion of relative stability, but this could be due to larger fitting error in the Val case. The shortest Trp-Trp contacts are for the W2W11 structure, which is also the most stable. In addition, the relative alignment of Trp-Trp in WYYW is somewhat different from that in the other three hairpins, which may be a source of its reduced stability. By contrast, the secondary structure (strand formation, from IR T_m values) has about the same stability in both mutations, especially considering fitting errors. This deviation of tertiary and secondary stabilities may indicate that specific Trp/Trp edge-to-face interactions could be reduced by effects of electronic coupling to other neighboring aromatic (Tyr) residues or by steric interferences. In other words, all adjacent aromatic pairs appear to interact together and result in a coupled unfolding mechanism.

Efficacy of Aromatic Interactions to Protein Stability. All mutants with one Trp/Trp pair having an edge-to-face interaction have similar T_m values for secondary structure stability, whether the pair is at either the termini of the β-strands or near the β-turn, with the possible exception of W4W9, which is subject to added fraying at the termini. This implies that putting a stable Trp/Trp pair at the termini of the β-strand can help peptides to form more extended β strands, but this will not necessarily improve backbone thermal stability since the formation of a tight turn stresses the strand alignment which then relaxes (distort) unless stabilized by other interactions. In contrast, a systematically designed tertiary aromatic interaction group can stabilize the secondary structure more efficiently, as evidenced by WYWY, whose IR thermal variation yields a much higher T_m, being stabilized by two pairs of Trp/Tyr edge-to-face interactions coupled through one Trp/Trp face-to-face pair. Structurally, this is evidenced by hairpin formation with a flatter, more extended β-strand interaction. Of course, TZ2 has an even higher stability due to having two Trp/Trp pairs. Finally, the Tyr mutants WYYW and YWWY have T_m values similar to those of the Val mutants W2W11 and W4W9, which indicates that a Tyr/Tyr aromatic interaction does not provide an added contribution

to secondary structure stability as compared to a Val-Val hydrophobic interaction.

Simulations involving these tertiary aromatic interaction geometries (edge-to-face, parallel-displaced, and face-to-face) in Trpzip2 have been reported by the Brooks group (*16*). They also showed the edge-to-face geometry to be more favorable, which was there attributed to high electrostatic multipole interaction energy. Consistent with work from other groups (*14*, *26*, *60*), our study details specific tryptophan-related aromatic interaction geometries, which result in corresponding CD patterns characteristic of interacting pairs of aromatic residues. In addition, this work incorporates selected aromatic residues into a model β-hairpin in order to study the effect of tertiary hydrophobic interactions on secondary structure stability at various positions and with different interaction geometries.

ACKNOWLEDGMENT

We thank Ben Ramirez from the UIC Structural Biology Center for assistance with the NMR experiments and Anjan Roy for carrying out test TD-DFT calculations.

SUPPORTING INFORMATION AVAILABLE

Details of the NMR chemical shift assignment and comparative analyses of the CD and IR thermal data with different models. This material is available free of charge via the Internet at http://pubs.acs.org.

REFERENCES

1. Cochran, A. G., Skelton, N. J., and Starovasnik, M. A. (2001) Tryptophan zippers: stable, monomeric beta-hairpins. *Proc. Nat. Acad. Sci. U.S.A. 98*, 5578–5583.
2. Searle, M. S., and Ciani, B. (2004) Design of β-sheet systems for understanding the thermodynamics and kinetics of protein folding. *Curr. Opin. Struct. Biol. 14*, 458–464.
3. Aravinda, S., Shamala, N., Roy, R. S., and Balaram, P. (2003) Non-protein amino acids in peptide design. *Proc. Indian Acad. Sci.* (*Chem. Sci.*) *115*, 373–400.
4. Venkatraman, J., Shankaramma, S. C., and Balaram, P. (2001) Design of folded peptides. *Chem. Rev. 101*, 3131–3152.
5. Balaram, P. (1999) De novo design: backbone conformational constraints in nucleating helices and β-hairpins. *Chem. Rev. 54*, 195–199.
6. Gellman, S. H. (1998) Minimal model systems for β-sheet secondary structure in proteins. *Curr. Opin. Struct. Biol. 2*, 717–725.
7. Dyer, R. B., Maness, S. J., Peterson, E. S., Franzen, S., Fesinmeyer, R. M., and Andersen, N. H. (2004) The mechanism of β-hairpin formation. *Biochemistry 43*, 11560–11566.
8. Kuznetsov, S. V., Hilario, J., Keiderling, T. A., and Ansari, A. (2003) Spectroscopic studies of structural changes in two β-sheet-forming peptides show an ensemble of structures that unfold noncooperatively. *Biochemistry 42*, 4321–4332.
9. Espinosa, J. F., Syud, F. A., and Gellman, S. H. (2002) Analysis of the factors that stabilize a designed two-stranded antiparallel β-sheet. *Protein Sci. 11*, 1492–1505.
10. Jager, M., Nguyen, H., Crane, J. C., Kelly, J. W., and Gruebele, M. (2001) The folding mechanism of a β-sheet: the WW domain. *J. Mol. Biol. 311*, 373–393.
11. Jourdan, M., Griffiths-Jones, S. R., and Searle, M. S. (2000) Folding of a β-hairpin peptide derived from the N-terminus of ubiquitin. *Eur. J. Biochem. 267*, 3539–3548.
12. Griffiths-Jones, S. R., Maynard, A. J., and Searle, M. S. (1999) Dissecting the stability of a β-hairpin peptide that folds in water: NMR and molecular dynamics analysis of the β-turn and β-strand contributions to folding. *J. Mol. Biol. 292*, 1051–1069.
13. Munoz, V., Thompson, P. A., and Hofrichter, J. (1997) Folding dynamics and mechanism of beta-hairpin formation. *Nature 390*, 196–199.
14. Mahalakshmi, R., Raghothama, S., and Balaram, P. (2006) NMR analysis of aromatic interactions in designed peptide β-hairpins. *J. Am. Chem. Soc. 128*, 1125–1138.
15. Chelli, R., Gervasio, F. L., Procacci, P., and Schettino, V. (2002) Stacking and t-shape competition in aromatic-aromatic amino acid interactions. *J. Am. Chem. Soc. 124*, 6133–6143.
16. Guvench, O., and Brooks, C. L., III (2005) Tryptophan side chain electrostatic interactions determine edge-to-face vs parallel-displaced tryptophan side chain geometries in the designed β-hairpin "trpzip2. *J. Am. Chem. Soc. 127*, 4668–4674.
17. Samanta, U., Pal, D., and Chakrabarti, P. (1999) Packing of aromatic rings against tryptophan residues in proteins. *Acta Crystallogr., Sect. D 55*, 1421–1427.
18. Chou, P. Y., and Fasman, G. D. (1978) Prediction of the secondary structure of proteins from their amino acid sequence. *Adv. Enzymol. 47*, 45–148.
19. Hughes, R. M., and Waters, M. J. (2006) Arginine methylation in a β-hairpin peptide: implications for Arg-π interactions, ΔCp°, and the cold denatured state. *J. Am. Chem. Soc. 128*, 12735–12742.
20. Jackups, R. J., and Liang, J. (2005) Interstrand pairing patterns in β-barrel membrane proteins: the positive outside rule, aromatic rescue, and strand registration prediction. *J. Mol. Biol. 354*, 979–993.
21. Jiang, B., Guo, T., Peng, L.-W., and Sun, Z.-R. (1998) Folding type-specific secondary structure propensities of amino acids, derived from α-helical, β-sheet, α/β, and $\alpha_+ \beta$ proteins of known strucure. *Biopolymers 45*, 35–49.
22. Mandel-Gutfreund, Y., Zaremba, S. M., and Gregoret, L. M. (2001) Contributions of residue pairing to β-sheet formation: conservation and covariation of amino acid residue pairs on antiparallel β-strands. *J. Mol. Biol. 305*, 1145–1159.
23. Merkel, J. S., and Regan, L. (1998) Aromatic rescue of glycine in β-sheets. *Fold Des. 3*, 449–455.
24. Steward, R. E., and Thornton, J. M. (2002) Prediction of strand pairing in antiparallel and parallel β-sheets using information theory. *Proteins: Struct., Funct., Genet. 48*, 178–191.
25. Wouters, M. A., and Curmi, P. M. G. (1995) An analysis of side chain interactions and pair correlations within antiparallel β-sheets: the difference between backbone hydrogen-bonded and non-hydrogen-bonded residue pairs. *Proteins: Struct., Funct., Genet. 22*, 119–131.
26. Jager, M., Dendle, M., Fuller, A. A., and Kelly, J. W. (2007) A cross-strand Trp-Trp pair stabilizes the hPin1 WW domain at the expense of function. *Protein Sci. 16*, 2306–2313.
27. Eidenschink, L., Kier, B. L., Huggins, K. N. L., and Andersen, N. H. (2009) Very short peptides with stable folds: Building on the interrelationship of Trp/Trp, Trp/cation, and Trp/backbone-amide interaction geometries. *Proteins: Struct., Funct., Bioinf. 75*, 308–322.
28. Eidenschink, L., Crabbe, E., and Andersen, N. H. (2009) Terminal sidechain packing of a designed β-hairpin influences conformation and stability. *Biopolymers 91*, 557–564.
29. Butterfield, S. M., Cooper, W. J., and Waters, M. L. (2005) Minimalist protein design: a β-hairpin peptide that binds ssDNA. *J. Am. Chem. Soc. 127*, 24–25.
30. Andersen, N. H., Olsen, K. A., Fesinmeyer, R. M., Tan, X., Hudson, F. M., Eidenschink, L. A., and Farazi, S. R. (2006) β-hairpin minimization and optimization. *J. Am. Chem. Soc. 128*, 6101–6110.
31. Tatko, C. D., and Waters, M. L. (2004) Comparison of C-H...π and hydrophobic interactions in a β-hairpin peptide: impact on stability and specificity. *J. Am. Chem. Soc. 126*, 2028–2034.
32. de Alba, E., Jimenez, M. A., Rico, M., and Nieto, J. L. (1996) Conformational investigation of designed short linear peptides able to form into β-hairpin structures in aqueous solution. *Fold Des. 1*, 133–144.
33. Dyer, R. B., Maness, S. J., Franzen, S., Fesinmeyer, R. M., Olsen, K. A., and Andersen, N. H. (2005) Hairpin folding dynamics: the cold-denatured state is predisposed for rapid refolding. *Biochemistry 44*, 10406–10415.
34. Andersen, N. H., dyer, R. B., Fesinmeyer, R. M., Gai, F., Liu, Z., Neidigh, J. W., and Tong, H. (1999) Effect of hexafluorosiopropanol on the thermodynamics of peptide secondary structure formation. *J. Am. Chem. Soc. 121*, 9879–9880.
35. Maynard, A. J., Sharman, G. J., and Searle, M. S. (1998) Origin of β-hairpin stability in solution: structural and thermodynamic analysis of the folding of a model peptide supports hydrophobic stabilization in water. *J. Am. Chem. Soc. 120*, 1996–2007.
36. Fesinmeyer, R. M., Hudson, F. M., and Andersen, N. H. (2004) Enhanced hairpin stability through loop design: the case of the protein G B1 hairpin. *J. Am. Chem. Soc. 126*, 7238–7243.
37. Kobayashi, N., Honda, S., Yoshii, H., and Munekata, E. (2000) Role of side-chains in the cooperative β-hairpin folding of the short C-terminal fragment derived from streptococcal protein G. *Biochemistry 39*, 6564–6571.
38. Kiehna, S. E., and Waters, M. J. (2003) Sequence dependence of β-hairpin structure: Comparison of a salt bridge and an aromatic interaction. *Protein Sci. 12*, 2657–2667.

39. Espinosa, J. F., Munoz, V., and Gellman, S. H. (2001) Interplay between hydrophobic cluster and loop propensity in β-hairpin formation. *J. Mol. Biol. 306*, 397–402.
40. Wu, L., McElheny, D., Huang, R., and Keiderling, T. A. (2009) Role of Trp-Trp interactions in Trpzip β-hairpin formation, structure and stability. *Biochemistry 48*, 10362–10371.
41. Huang, R., Wu, L., McElheny, D., Bour, P., Roy, A., and Keiderling, T. A. (2009) Cross-strand coupling and site-specific unfolding thermodynamics of a Trpzip β-hairpin peptide using 13C isotopic labeling and IR spectroscopy. *J. Phys. Chem. B 113*, 5661–5674.
42. Hauser, K., Krejtschi, C., Huang, R., Wu, L., and Keiderling, T. A. (2008) Site-specific relaxation kinetics of a tryptophan zipper hairpin peptide using temperature-jump IR spectroscopy and isotopic labeling. *J. Am. Chem. Soc. 130*, 2984–2992.
43. Takekiyo, T., Wu, L., Yoshimura, Y., Shimizu, A., and Keiderling, T. A. (2009) Relationship between hydrophobic interactions and secondary structure stability for Trpzip β-hairpin peptides. *Biochemistry 48*, 1543–1552.
44. Delaglio, F., Grzesiek, S., Vuister, G. W., Zhu, G., Pfeifer, J., and Bax, A. (1995) NMRRipe: A multidimensional spectral processing system based on UNIX pipes. *J. Biomol. NMR 6*, 277–293.
45. Johnson, B. A., and Blevins, R. A. (1994) NMR View: A computer program for the visualization and analysis of NMR data. *J. Biomol. NMR 4*, 604–613.
46. Hwang, T., and Shaka, A. J. (1995) Water suppression that works: excitation sculpting using arbitrary waveforms and pulsed field gradients. *J. Magn. Reson. 112A*, 275–279.
47. Guntert, P., Mumenthaler, C., and Wuthrich, K. (1997) Torsion angle dynamics for NMR structure calculation with the new program DYANA. *J. Mol. Biol. 273*, 283–298.
48. DeGuzman, R. N., Goto, N. K., Dyson, H. J., and Wright, P. E. (2006) Structural basis for cooperative transcription factor binding to the CBP coactivator. *J. Mol. Biol. 355*, 1005–1013.
49. Hornak, V., Abel, R., Okur, A., Strockbine, B., Roitberg, A., and Simmerling, C. (2006) Comparison of multiple Amber force fields and development of improved protein backbone parameters. *Proteins: Struct., Funct., Bioinf. 65*, 712–725.
50. Osapay, K., and Case, D. A. (1991) A new analysis of proton chemical shifts in proteins. *J. Am. Chem. Soc. 113*, 9436–9444.
51. Laskowski, R. A., Rullmann, J. A. C., MacArthur, M. W., Kaptein, R., and Thornton, J. M. (1999) AQUA and PROCHECK-NMR: programs for checking the quality of protein structures solved by NMR. *J. Biomol. NMR 8*, 477–486.
52. Fesinmeyer, R. M., Hudson, F. M., Olsen, K. A., White, G. W., Euser, A., and Andersen, N. H. (2005) Chemical shifts provide fold populations and register of β hairpins and β sheets. *J. Biomol. NMR 33*, 213–231.
53. Syud, F. A., Stanger, H. E., Mortell, H. S., Espinosa, J. F., Fisk, J. D., Fry, C. G., and Gellman, S. H. (2003) Influence of strand number on antiparallel β-sheet stability in designed three- and four-stranded β-sheets. *J. Mol. Biol. 326*, 553–568.
54. Syud, F. A., Stranger, H. E., and Gellman, S. H. (2001) Interstrand side chain-side chain interactions in a designed β-hairpin: significance of both lateral and diagonal pairings. *J. Am. Chem. Soc. 123*, 8667–8677.
55. Sharman, G. J., Griffiths-Jones, S. R., Jourdan, M., and Searle, M. S. (2001) Effects of amino acid φ,ψ propensities and secondary structure interactions in modulating Hα chemical shifts in peptide and protein β-sheet. *J. Am. Chem. Soc. 123*, 12318–12324.
56. Blanco, F. J., Jimenez, M. A., Pineda, A., Rico, M., Santoro, J., and Nieto, J. L. (1994) NMR solution structure of the isolated N-terminal fragment of protein-G B1 domain. Evidence of trifluoroethanol induced native-like β-hairpin formation. *Biochemistry 33*, 6004–6014.
57. Cochran, A. G., Skelton, N. J., and Starovasnik, M. A. (2002) Correction. *Proc. Natl. Acad. Sci. U.S.A. 99*, 9081–9082.
58. Roy, A., Bour, P., and Keiderling, T. A. (2009) TD-DFT modeling of the circular dichroism for a tryptohan zipper peptide with coupled aromatic residues. *Chirality 21*, E163–E171.
59. Kubelka, J., and Keiderling, T. A. (2001) Differentiation of β-sheet forming structures: ab initio based simulations of IR absorption and vibrational CD for model peptide and protein β-sheets. *J. Am. Chem. Soc. 123*, 12048–12058.
60. Kier, B. L., and Andersen, N. H. (2008) Probing the lower size limit for protein-like fold stability: ten-residue microproteins with specific, rigid structures in water. *J. Am. Chem. Soc. 130*, 14675–14683.